Mechanical Behavior of Additive Manufactured Layered Materials, Part 2: Stainless Steels*

Todd M. Mower† and Michael J. Long

M.I.T. Lincoln Laboratory

244 Wood Street

Lexington, MA 02420

†Corresponding author; mower@ll.mit.edu

* This work is sponsored by the Department of the Air Force under the United States Air Force contract number FA8721-05-C-0002. The opinions, interpretations, recommendations and conclusions are those of the authors and are not necessarily endorsed by the United States Government.

Abstract

Mechanical behavior of two stainless steel alloys produced with Direct Metal Laser Sintering (DMLS) was measured and is compared to that of similar conventional materials. Flexural modulus measurements were obtained, tensile deformation characterization was performed, and fatigue behavior was investigated in fully reversed bending. Compared to wrought and annealed materials, DMLS 316L demonstrated significantly higher yield strength but similar strain hardening and strain to failure, whereas DMLS 17-4PH exhibited lower yield strength. Fatigue specimens produced additively in the horizontal orientation, such that cyclic stresses were applied in the direction parallel to build planes, displayed fatigue strengths of approximately 85% (316L) to 95% (17-4PH) of that of wrought, annealed material. Fatigue behavior was diminished drastically when DMLS specimens (fabricated vertically) were stressed across the build planes. Vertically-built 316L specimens subjected to hot isostatic pressure demonstrated improved cyclic fatigue strength. In all the additive materials, fatigue cracks initiated at surface defects, internal voids and pre-existing microcracks.

Keywords: SS316L, SS17-4PH, DMLS, fatigue, light microscopy, powder bed fusion,

1. Introduction

1.1 Background

Additive manufacturing (AM) technologies are increasingly being used to fabricate complex structural components used in fielded systems. The most prevalent systems utilize lasers to fuse incrementally deposited, pre-alloyed powder, creating three dimensional structures according to digitally-defined geometries [1]. Methods to additively manufacture materials with either selective laser melting (SLM) or direct metal laser sintering (DMLS) have recently been termed as "powder bed fusion" processes by ASTM International [2].

Characterization of the mechanical properties of additive, layered materials produced by laser-heating methods has not kept pace with the proliferation of the systems put into service. In the first part of this article, measured mechanical behaviors of powder-bed fusion-produced AlSi10Mg and Ti6Al4V were presented. A few other reports concerning the mechanical behavior of additive AlSi10Mg [3,4,5,6] and Ti6Al4V [7,8,9,10,11,12] have been published recently, but published reports concerning mechanical properties of stainless steels produced with powder-bed fusion techniques are much more limited.

Rafi et al.[13] and Spierings et al.[14] both included stainless steel (SS) 15-5 in their studies of mechanical properties of DMLS materials. Investigations of the microstructure [15] and fatigue-crack growth rates [16] in SS316L produced with SLM have been reported. Spierings et al. also measured fatigue strengths of SLM 316L, under tensile loading with load ratio of R=0.1. Most recently, Murr et al. have described very detailed studies of the microstructures of 17-4PH materials produced with SLM, relating hardness of the materials to the type of gas used in the SLM chamber, but no other mechanical property measurements were reported [17].

1.2 Scope of the current work

This study was executed to contribute to the understanding of the mechanical behavior of stainless steels produced using commercially-available, powder-bed fusion methods. The two materials studied have often been used (in wrought, machined form) in applications requiring high strength, corrosion resistance and/or excellent cyclic fatigue behavior: stainless-steel 316L and 17-4PH. Additive materials were fabricated at a leading-edge facility using their typical process parameters, with specimens produced in two different build orientations. Flexural moduli, stress-strain behaviors and fatigue strengths were measured. Reference material behaviors were obtained from conventional counterparts, i.e. specimens machined from wrought materials.

Examinations of material microstructures were performed to reveal grain sizes, solidification morphology and prevalence of interior voids within the additive materials. Optical microscopy and profilometry were used to measure surface roughness and to characterize intrinsic defects, which are shown to have direct bearing on fatigue strength.

Tensile deformation measurements are presented in stress-strain plots, emphasizing the differences in yield and post-yield behaviors between conventional materials and the corresponding DMLS materials. Measured fatigue-strength data are presented in traditional S-N plots, including wrought and machined specimens to provide a reference or "baseline." Fatigue behaviors of the AM specimens are compared to those of conventional materials, and are considered in relation to intrinsic defects observed on the exterior surfaces and revealed within the interior, on fracture surfaces.

2. Experimental details

2.1 Powder-bed material fabrication

The two SS materials (316L and 17-4PH) studied were fabricated using an EOS M270, a direct metal laser sintering (DMLS) system. Raw material powders were obtained from EOS GmbH, and was Nadcap[1] certified with particle sizes ranging from 15 to 45 µm. The build chamber was backfilled with nitrogen gas, while powder melting and fusion was performed with a 195W laser with a spot size of 100 µm, travelling at 750 mm/s. Specimens were built on a plate maintained at 82°C, with layer thicknesses of approximately 40 and 20 µm for the 316L and 17-4PH, respectively. Thermal stress relieving was performed prior to removing specimens from the build platforms: 316L specimens were held at 388ºC for four hours; 17-4PH specimens were soaked at 788°C for one hour.

2.2 Specimen preparation

Tensile specimens were contoured to dimensions consistent with ASTM Standard E8-09, as detailed in a drawing included in Part 1 of this article, and shown below in Figure 1. DMLS tensile specimens were produced in both horizontal orientation (specimens on edge) and inclined at a 45-degree angle (specimens were too long to stand vertically in the build chamber). Specimens of "conventional material" were machined from wrought, rolled sheet stock of certified 316L and 17-4PH obtained in the mill-annealed condition, with the tensile axis aligned with the plate roll direction (longitudinal). All surfaces of the DMLS tensile specimens were left in the as-fabricated condition, while the conventional materials were machined and finished to a surface roughness of ~0.8 µm, rms.

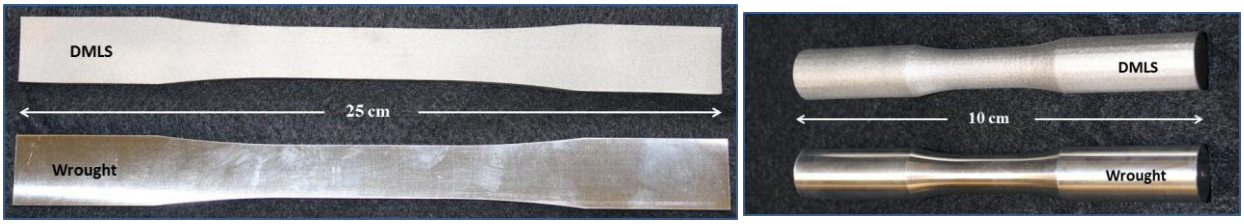

**Figure 1: Left, tensile specimens with plate thickness ~ 3.8 mm.
Right, fatigue specimens with diameter ~ 12.5 mm.**

[1] Nadcap (formerly NADCAP, the National Aerospace and Defense Contractors Accreditation Program).

The fatigue specimens used in this study were axisymmetric cylinders, also shown in Figure 1, contoured in an "hourglass" shape with a reduced diameter in the central section. DMLS fatigue specimens were produced in both horizontal and vertical orientations. Note that horizontal specimens have the tensile axis parallel to the build planes, while vertical specimens have the tensile axis perpendicular to build planes. The contoured surfaces were not machined but were left in the condition produced by the additive manufacturing process. Conventional specimens were machined from wrought, rolled bar stock of certified SS316L and 17-4PH in the annealed condition, and polished with successively finer grits of Emery paper.

2.3 Specimen surface characterization

Optical microscopy of DMLS SS 316L fatigue-specimen surfaces is shown in Figure 2. In the low-magnification photo of horizontally-built material (Fig. 2a), linear artifacts of the build process are evident parallel to the long axis of the specimen. Discrete bumps and a finely-scaled texture are seen clearly at higher magnification (Fig. 2b). Vertically-built materials display similar features (Figs. 2c and 2d), with a more coarsely scaled surface, and several pores which often link together, in vertical planes. Similar observations of rough features and artifacts due to the discrete, layered fabrication process are evident on the surfaces of 17-4PH specimens, as demonstrated by the photographs shown in Figure 4.

Surface roughness of the fatigue specimens was measured using an optical profilometer (Cybertechnologies CT-300) with a white-light confocal sensor having height resolution of approximately 35 nm and lateral resolution of about 2μm. Optical profilometry was utilized instead of a mechanical profilometer, to enable detection of small pits or fine cracks that might enable initiation of fatigue cracks. Three-dimensional images of typical surface profilometry obtained from measurements on 316L fatigue specimens are shown in Figure 3. Numerous crevasses and rough features are present, and the indicated peak-to-valley heights range from approximately 60 μm to over 100 μm for specimens built in either orientation. Similar graphical representations of surface topography are shown in Figure 5 for 17-4PH materials. The image from a wrought, machined and polished specimen displays a peak-to-valley range of about 6 μm, while the DMLS horizontally-built material exhibits significantly rougher texture, with a peak-to-valley range of over 40 μm.

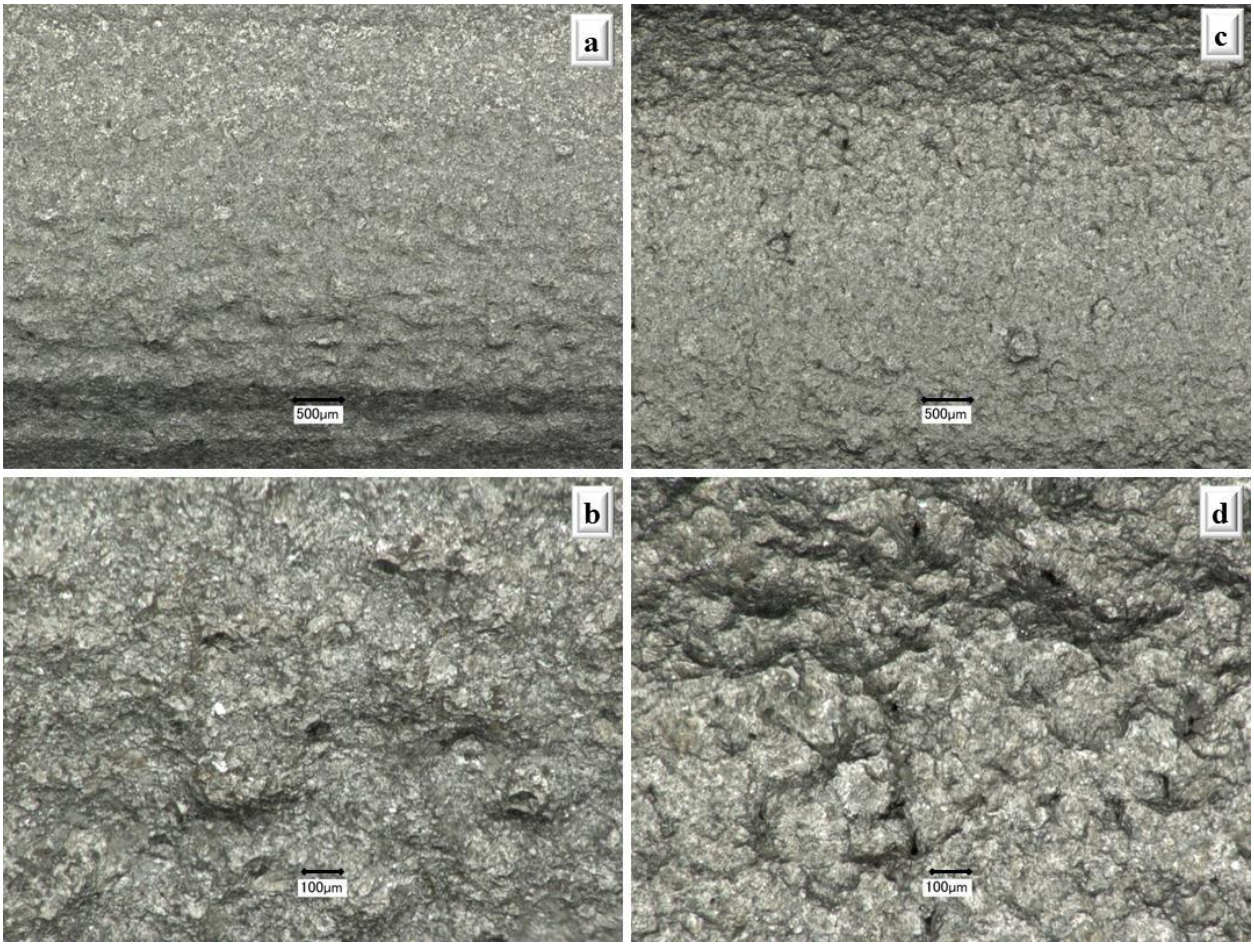

Figure 2: Optical microscopy of typical DMLS 316L fatigue-specimen surfaces. Horizontally-built, (a) and (b); vertically-built, (c) and (d).

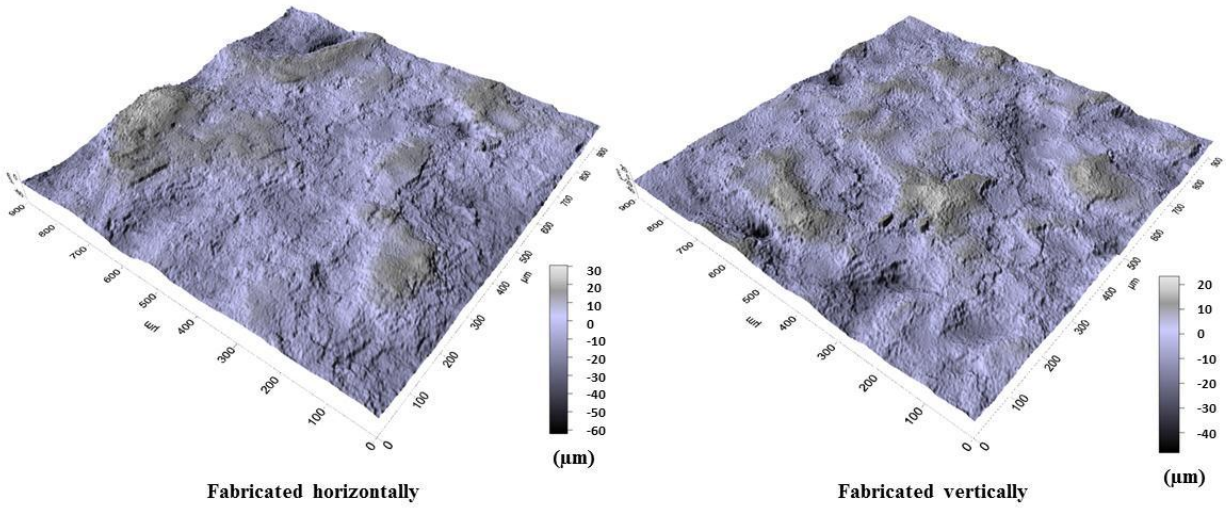

Figure 3: Surface maps from optical profilometry of DMLS SS316L fatigue specimens.

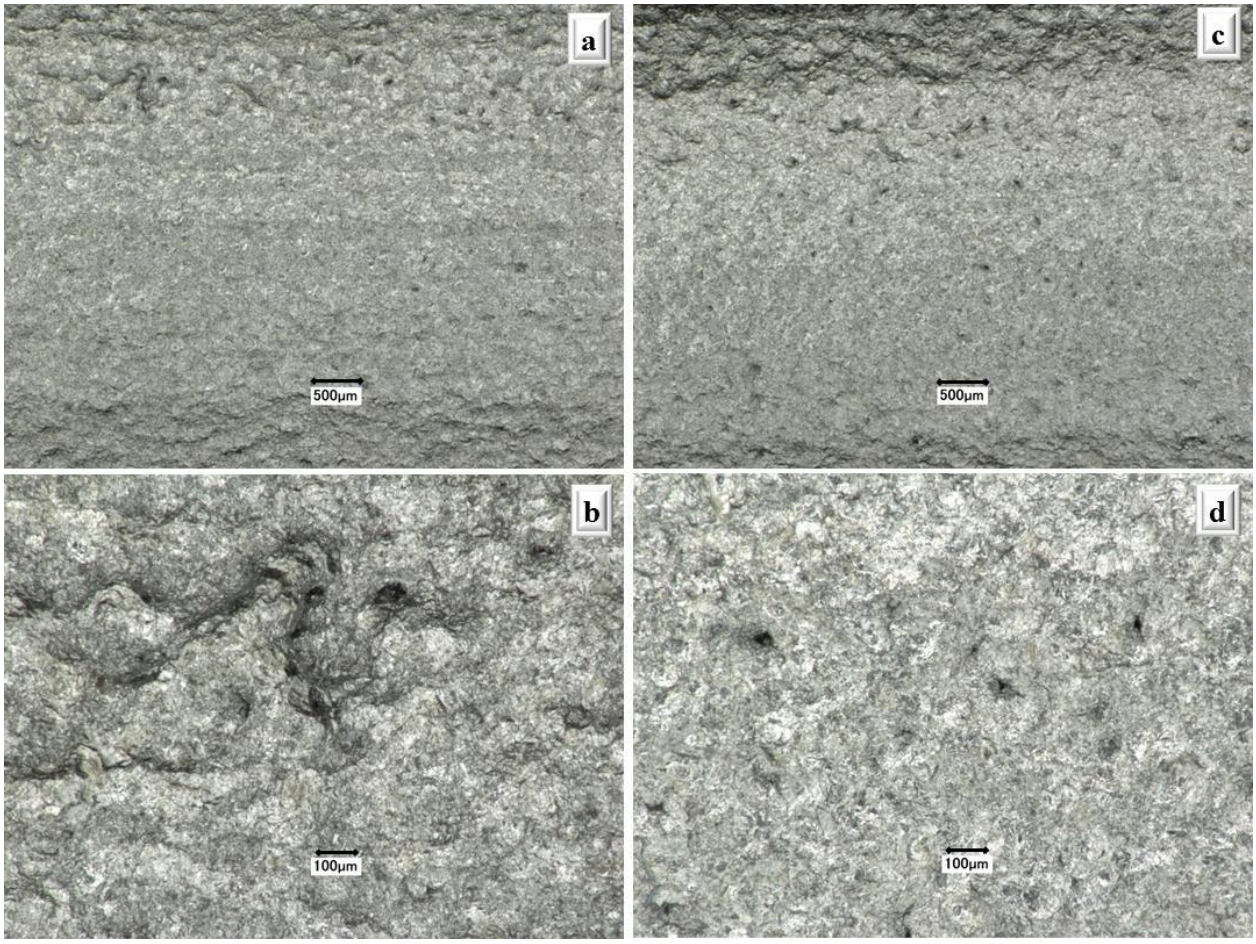

Figure 4: Optical microscopy of typical DMLS 17-4PH fatigue-specimen surfaces. Horizontally-built, (a) and (b); vertically-built, (c) and (d).

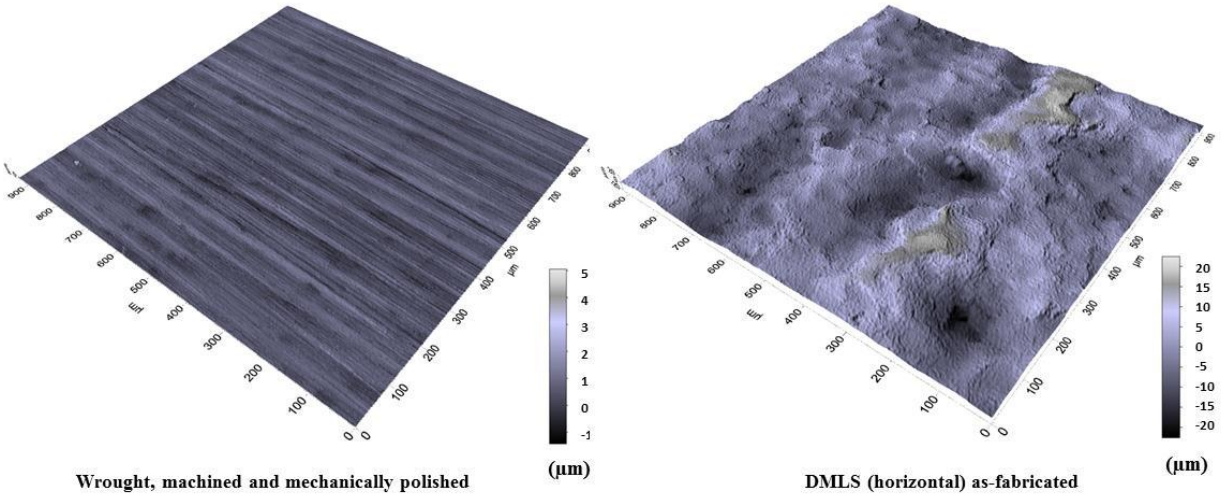

Figure 5: Surface maps from optical profilometry of 17-4PH fatigue specimens.

Presented in Table 1 are summaries of surface roughness measurements obtained from two fatigue specimens generated with each production technique. Specimens prepared with conventional techniques (machining and polishing with emery paper) resulted in surfaces with measured average roughness (S_a) of approximately 1 μm, with similar rms values. AM materials had significantly greater surface roughness. The measured surface roughness of DMLS 316L and 17-4PH fatigue specimens was approximately five times rougher than machined and polished specimens of wrought materials. In the first part of this article, evidence was presented showing the effectiveness of polishing AM surfaces (with mechanical and/or electrochemical methods) was limited, because as surface material is removed, subsurface voids become exposed.

Table 1: Roughness of fatigue specimen surfaces, measured with an optical profilometer.

Material	*Treatment*	S_a *(μm)*	S_{rms} *(μm)*
Conventional 316L	**Milled and polished**	**1**	**1**
DMLS 316L	**As fabricated**	**5 - 6**	**6 - 8**
Conventional 17-4PH	**Milled and polished**	**1**	**1**
DMLS 17-4PH	**As fabricated**	**3 - 5**	**4 - 7**

2.4 Microstructural analyses

Unstrained tensile specimens were sectioned transverse to the long axis to expose the microstructure of the materials studied. Thus, sections extracted from AM specimens fabricated in the horizontal orientation are perpendicular to the build plane. Sections were polished, etched with an electrolytic nitric-acid process, and examined with bright-field microscopy.

Sections of DMLS 316L materials (Fig. 6) show overlapping, segregated melt pools with distinct boundaries. The low-magnification photos show structures reminiscent of weld fillets, with voids more evident near free surfaces (where applied bending stresses would be highest). Higher magnification reveals a fine crystalline structure created by the rapid solidification of thin layers built upon previously solidified layers. Similar microstructures appear to have developed in the 316L materials fabricated in both the horizontal and inclined orientations.

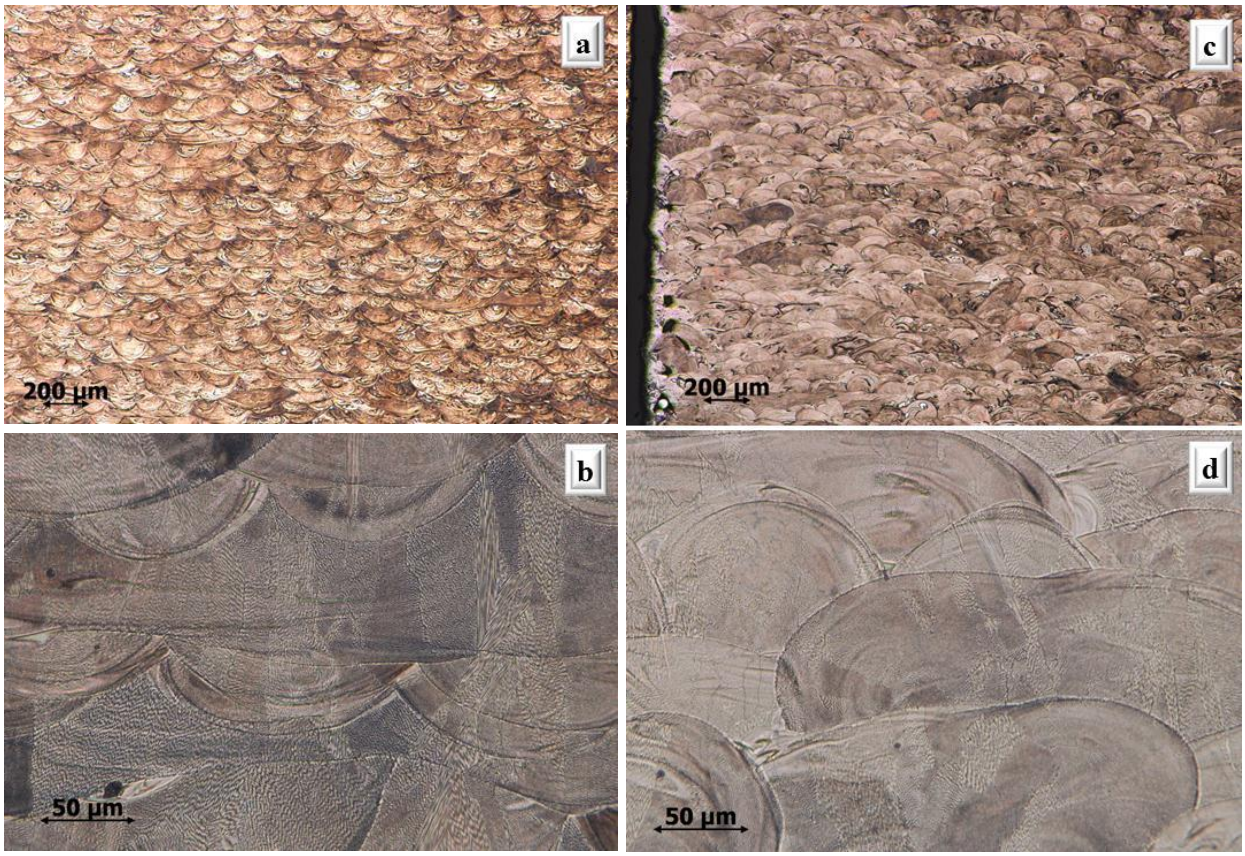

Figure 6: Microstructure of DMLS tensile specimens sectioned perpendicular to longitudinal axis. 316L built horizontally (a and b), and at a 45-degree incline (c and d).

Sections of DMLS 17-4PH materials built in the horizontal orientation (Fig. 7a,b) also show segregated melt pools with discrete boundaries, a few small voids and a very fine crystalline microstructure. The 17-4PH material built on an incline (Fig 7c,d) presents a very

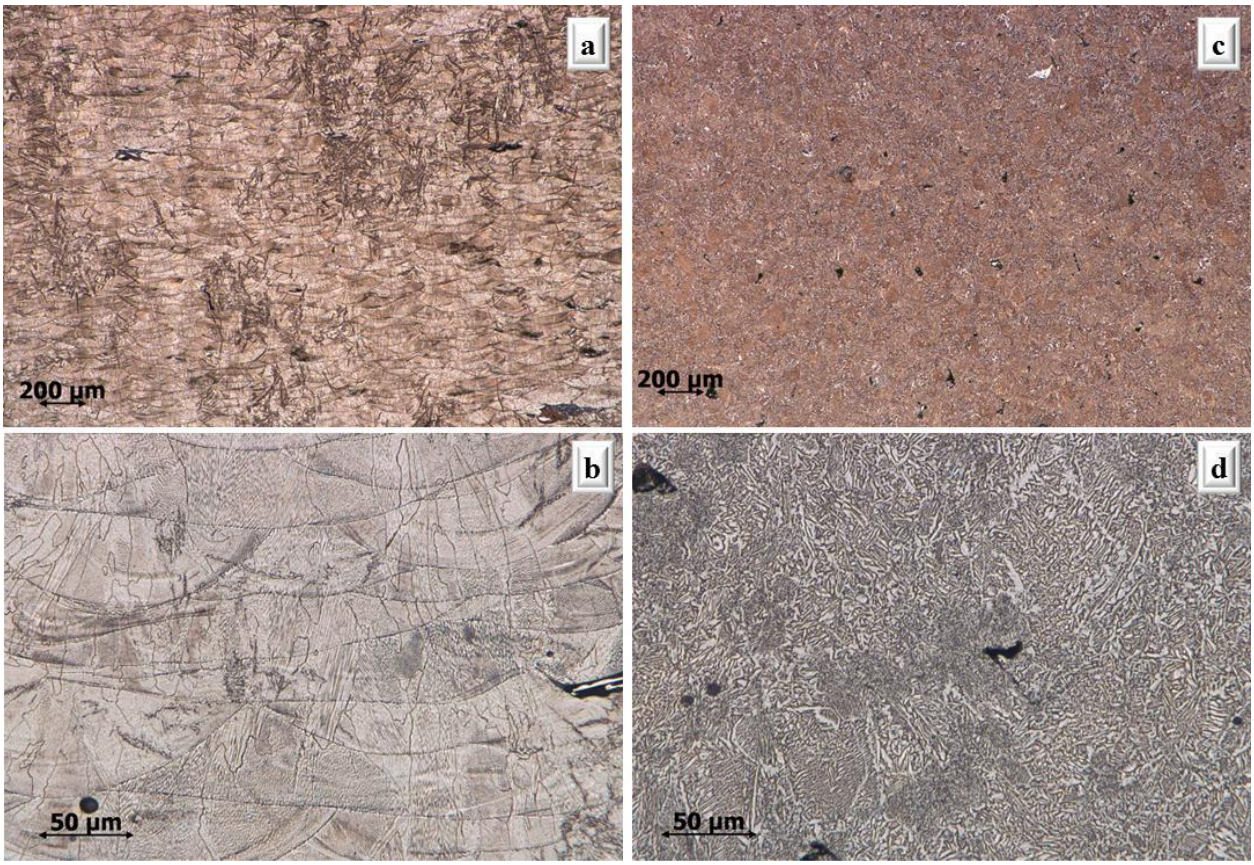

Figure 7: Microstructure of DMLS tensile specimens, sectioned perpendicular to longitudinal axis; 17-4PH built horizontally (a and b), and at a 45-degree incline (c and d).

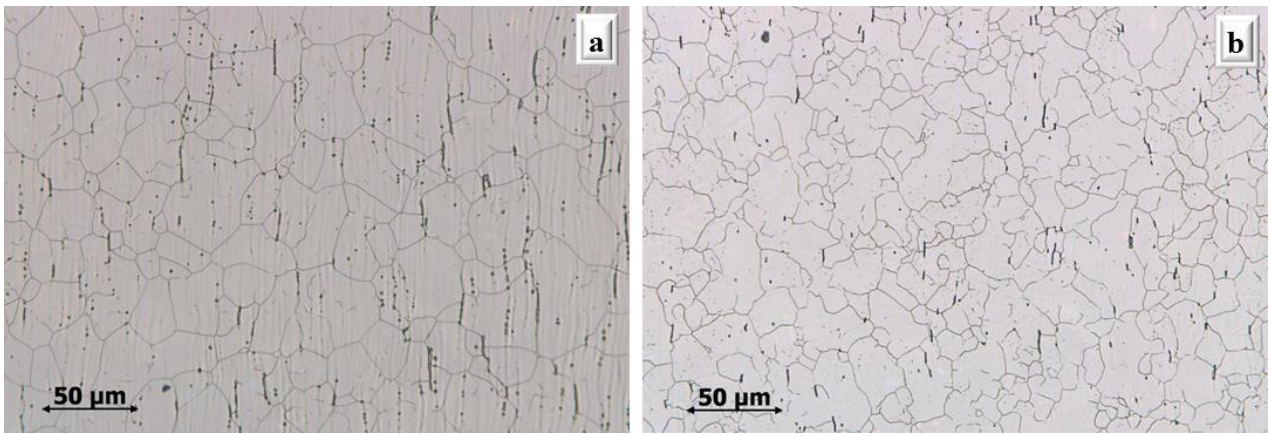

Figure 8: Microstructures of wrought materials: 316L (a) and 17-4PH (b).

different microstructure, with more numerous, larger voids, only faintly visible melt pools, and randomly-oriented lamellar colonies.

Microstructures of our wrought materials are shown in Figure 8. Grains in the 316L are nearly equiaxed, with sizes ranging from 15 to 55 μm. The microstructure of our wrought 17-4PH is similar, with noticeably smaller grain sizes ranging from 10 to 40 μm. Ferrite stringers are obvious in the 316L, aligned with the strains evident from the rolling process. Only a few stringers are evident in the 17-4PH, and no evidence of processing strain can be seen.

2.5 Flexural modulus

Flexural modulus measurements were conducted in a dynamic mechanical analyzer, at a frequency of 1 Hz, at ambient temperature. Details are provided in the first part of this article.

2.6 Tensile testing

Tensile stress-strain behavior was also measured at a strain rate of approximately 10^{-4}/s, at room temperature, and is also described in more detail in the first part of this article.

2.7 Fatigue testing procedures

Fatigue behavior was investigated in fully reversed, rotating beam mode at room temperature and with frequencies from 20 to 25Hz. Eight to twelve samples of each material studied were fatigue tested, in a "staircase" manner beginning with cyclic stress amplitudes just below the yield strength and then progressively lower until reaching stress amplitudes that produced lifetimes of 10E6 cycles or greater ("run-out").

3. Results

3.1 Flexural modulus

Results of our flexural modulus measurements are listed in Table 2. Both stainless-steel DMLS materials demonstrated stiffness nearly equal to that of conventional (wrought and machined) corresponding materials, with specimens fabricated in the inclined position exhibiting greater stiffness than specimens fabricated horizontally. The most notable difference is the modulus of horizontally-built 17-4PH (about 10% less than that of wrought material); this behavior was observed in the tensile measurements as well.

Table 2: Flexural modulus (GPa) of DMLS materials and wrought counterparts.

Material	*Long.*	*Horiz.*	*45º*
Wrought 316L	**191.3**		
DMLS 316L		**187.3**	**189.1**
Wrought 17-4PH	**193.9**		
DMLS 17-4PH		**172.2**	**192.9**

3.2 Tensile deformation

Representative engineering stress-strain data from measurements obtained with our stainless steel specimens are shown in Figure 9. The 316L specimens display well-defined yield points followed by strain hardening that continued until failure occurred. Ultimate strains in the wrought 316L exceeded 35%, while the DMLS materials demonstrated nearly the same ductility. The yield strength (0.2% offset) demonstrated by DMLS 316L was significantly higher (~40%) than that of wrought material, as seen in the stress-strain curves and the summary data listed in Table 3. Significant thinning associated with the high ductility of 316L transpired in all of the tensile testing with these materials. Shown in Figure 10 is an example of thinning in a DMLS specimen, with a failure surface displaying features of ductile rupture as well as some minor porosity that is present in this material in the as-fabricated condition.

All of the 17-4PH materials demonstrated less ductility than 316L but achieved significantly higher ultimate tensile strengths. Although the DMLS material fabricated in the horizontal orientation (and thus, tested with the principal stress aligned with the build planes) showed the lowest yield strength of the 17-4 materials, it displayed the highest strain hardening, such that it reached an ultimate strength nearly equal to that of the wrought material. The most ductility in the 17-4 materials was produced in the DMLS specimens fabricated such that they stood at 45° angle within the build chamber. A photo of the failure region of one of these specimens is shown in Figure 11, in which extensive thinning is evident. Higher magnification of the failure surface reveals both cleavage-like, planar facets as well as layers of porosity that are artifacts of the fabrication process.

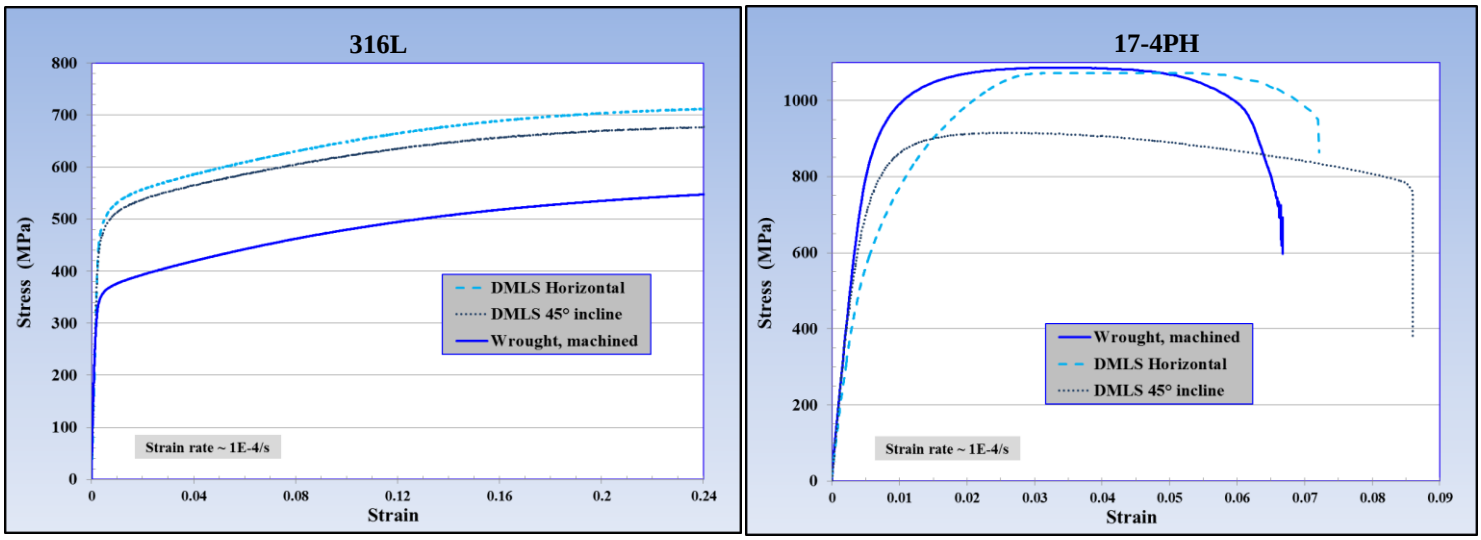

Figure 9: Measured room-temperature tensile deformation behavior of stainless steels produced with DMLS, compared to that of annealed, wrought and machined material.

Table 3: Average measured tensile properties of DMLS materials and wrought counterparts.

Material	*Orientation*	*Modulus (GPa)*	*Yield (MPa)*	*Ultimate (MPa)*	*Failure Strain*
Wrought 316L	**Longitudinal**	**187**	**345**	**563**	**>0.35**
DMLS 316L	**Horizontal**	**180**	**496**	**717**	**0.28**
DMLS 316L	**45° incline**	**193**	**473**	**680**	**0.31**
Wrought 17-4PH	**Longitudinal**	**186**	**898**	**1085**	**0.065**
DMLS 17-4PH	**Horizontal**	**165**	**610**	**1072**	**0.072**
DMLS 17-4PH	**45° incline**	**186**	**737**	**914**	**0.086**

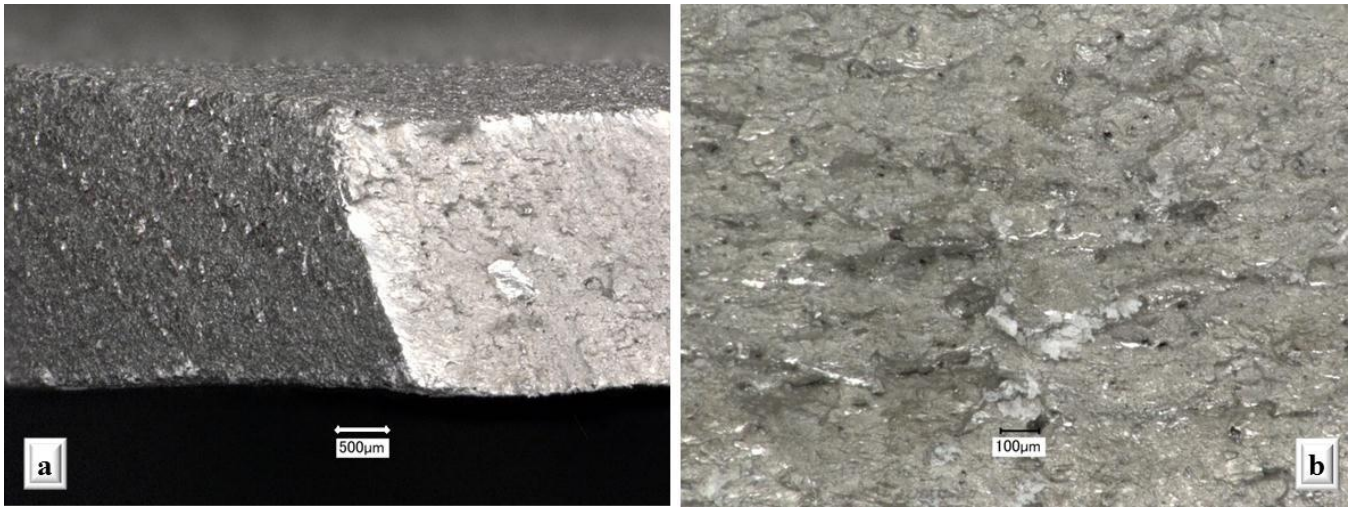

Figure 10: Failure surface of DMLS 316L tensile specimen fabricated horizontally; (a) thinning apparent due to high ductility, and (b) rough features of ductile fracture and minor, as-fabricated porosity.

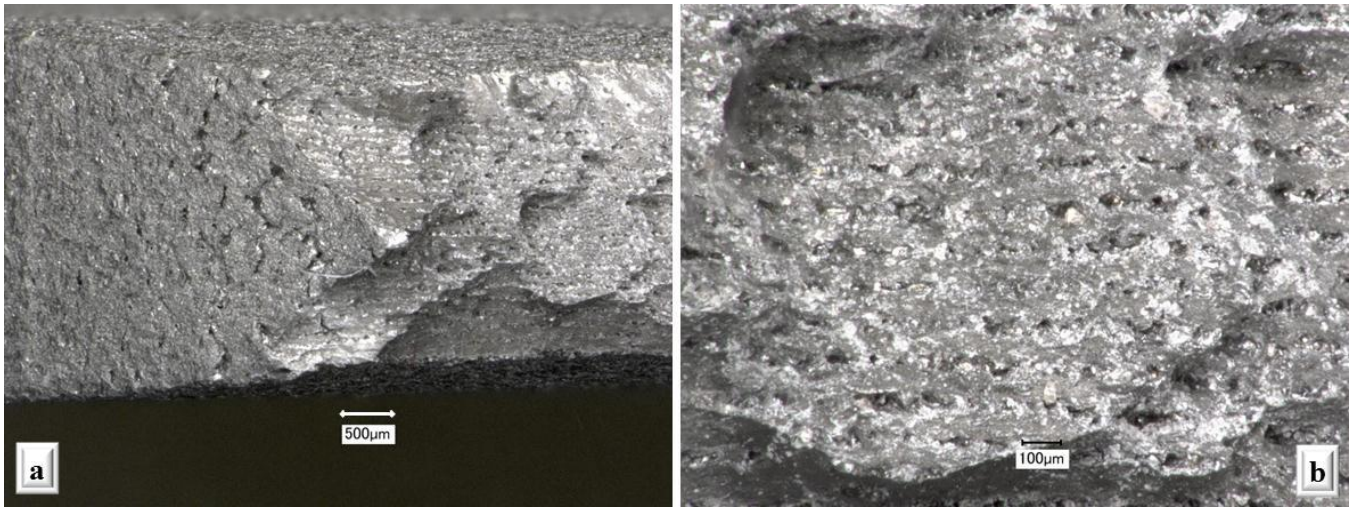

Figure 11: Failure surface of DMLS 17-4 tensile specimen fabricated standing at a 45° angle; (a) thinning and surface stretching, and (b) final rupture with cleavage-like features and stratified porosity.

3.3 Fatigue-strength measurements

Results from fatigue tests conducted with our SS316L specimens are plotted in Figure 12, in the form of a traditional S-N, or Wöhler diagram. The wrought and machined material displayed fatigue strengths above 350 MPa for lifetimes ranging from 10^5 to 10^6 cycles, progressively falling to an apparent endurance limit (10^7 cycles) of about 340 MPa. Specimens of DMLS materials fabricated in the horizontal orientation (and therefore subjected to bending stresses aligned with the build planes) produced fatigue strengths approximately 15% lower than those of the wrought material, with substantially higher scatter in the data. The first batch of DMLS specimens built in the vertical orientation (stressed across the build planes in the fatigue tests) produced such significantly lower fatigue strengths that we suspected a deviation in process parameters may have occurred during the production process. A second batch of vertically-built specimens produced identically poor fatigue strength. A third batch of vertically-built

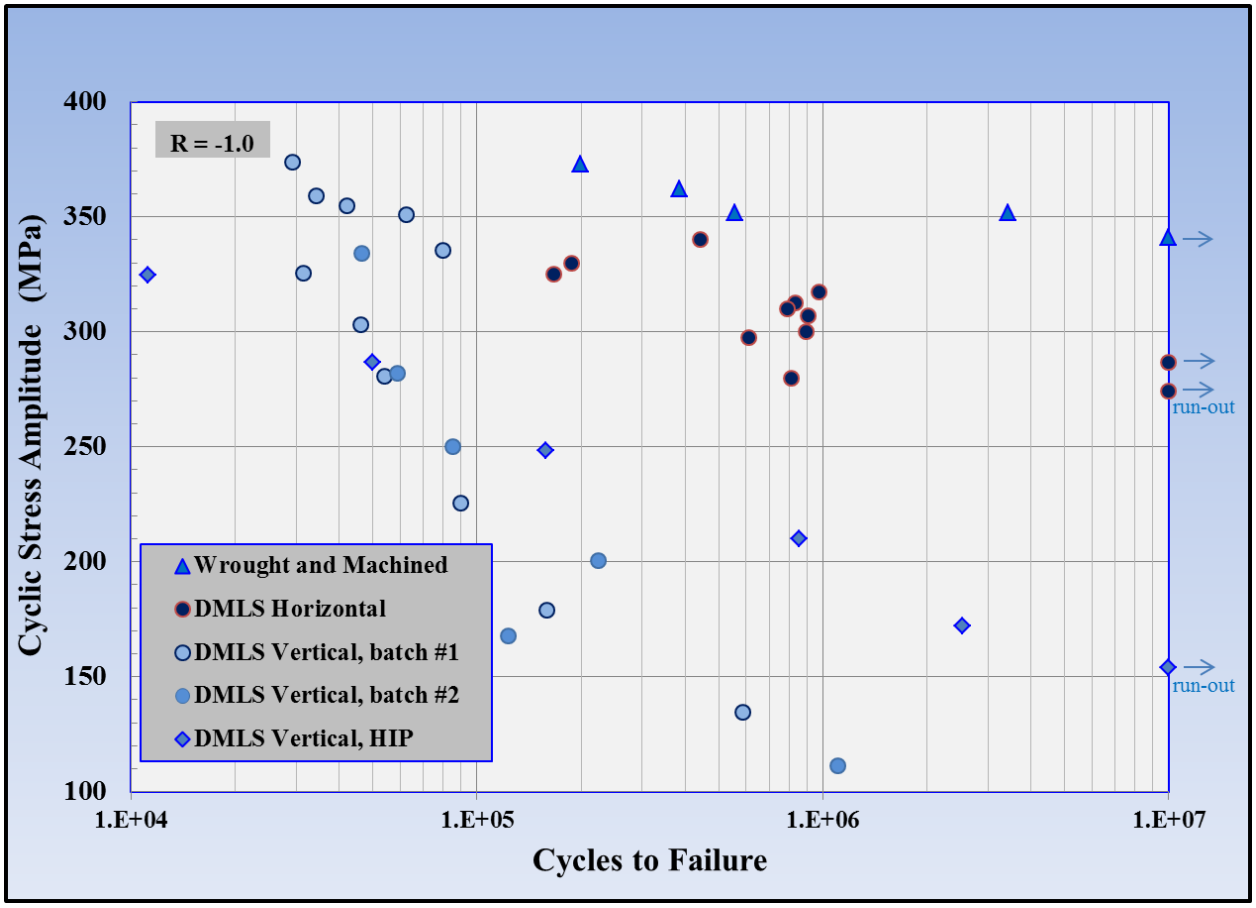

Figure 12: Measured room-temperature stress-life (S-N) of DMLS 316L, compared to that of conventional 316L. Bending fatigue (rotating beam) at a frequency of 25 Hz.

316L specimens was post-processed with hot isostatic pressure (HIP), at 1190°C and 145 MPa for four hours. This HIP process resulted in no improvement in low-cycle fatigue strength but did improve the high-cycle fatigue behavior, such that vertically-built, HIP'd material generated high-cycle fatigue strengths of approximately 50% of that of the horizontally-built materials.

Fatigue fractures of DMLS 316L materials produced in the horizontal orientation displayed rough features characteristic of ductile crack growth, as demonstrated by the example shown in Figure 13. In this case, the fatigue crack was initiated at a single dominant defect just beneath the surface. Other fractures of these materials incurred multiple fatigue cracks, all initiating at manufacturing defects upon or slightly beneath the surface.

The poor fatigue strengths exhibited by vertically-built DMLS 316L materials in this study is apparently due to an intrinsic low strength between build planes, as suggested by the nearly planar fracture surface shown in Figure 14a. Though fatigue cracks often were triggered by surface flaws, in this instance a cluster of interior voids provided the initiating defect. Trace evidence of the laser paths can be seen clearly upon this fracture surface, typical of all the vertically-built specimens. Additional evidence of incomplete fusion can be seen upon close examination of Figure 14b, in which beads of melted and solidified material can be seen trapped within voids between the laser paths.

Subjecting the vertically-built 316L to HIP appears to have more fully fused the material layers together, as evidenced by the fracture surface shown in Figure 15. This fractograph presents a surface that is non-planar and much rougher than those that occurred in non-HIP'd, vertically-built 316L. The fatigue fracture in this specimen intitated at multiple surface defects, rather than internal porosity, and no artifacts of the laser processing are evident.

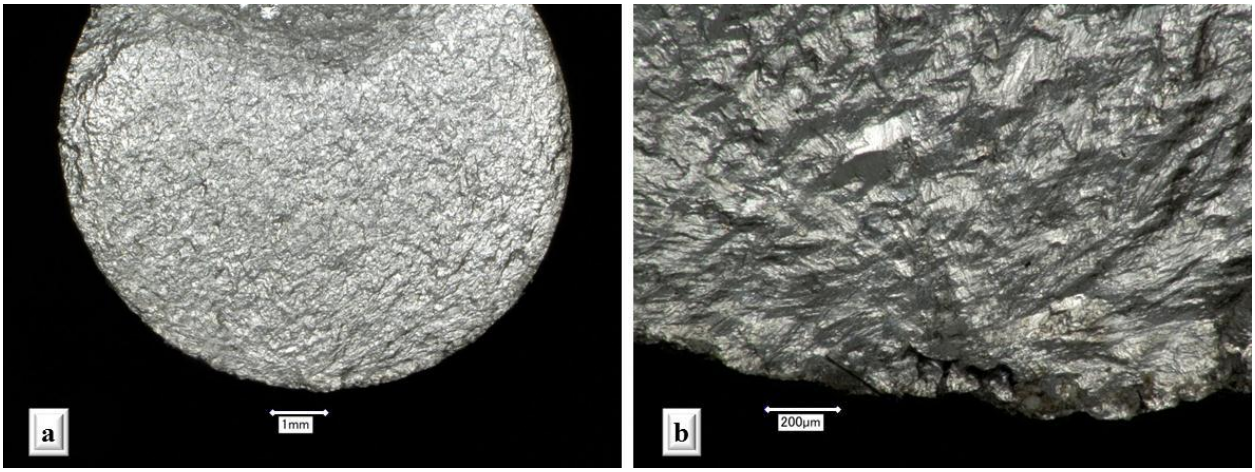

Figure 13: Fracture surface of horizontally-built DMLS 316L fatigue specimen; (a) ductile crack growth from one edge, initiating at (b) large subsurface cavity near rough surface features.

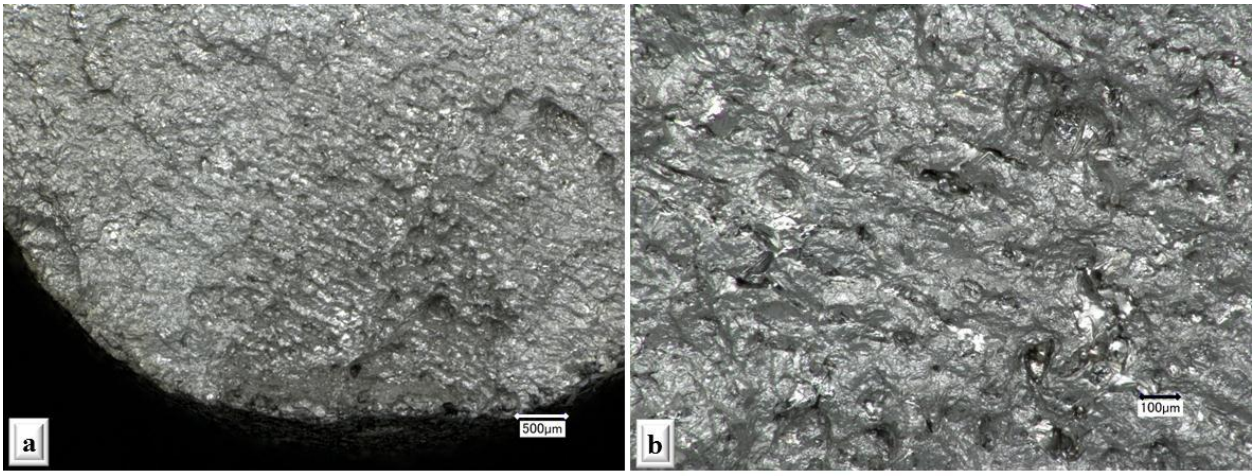

Figure 14: Fracture surface of vertically-built DMLS 316L fatigue specimen; (a) almost planar surface with voids near origin, (b) laser traces and beads of re-solidified material evident.

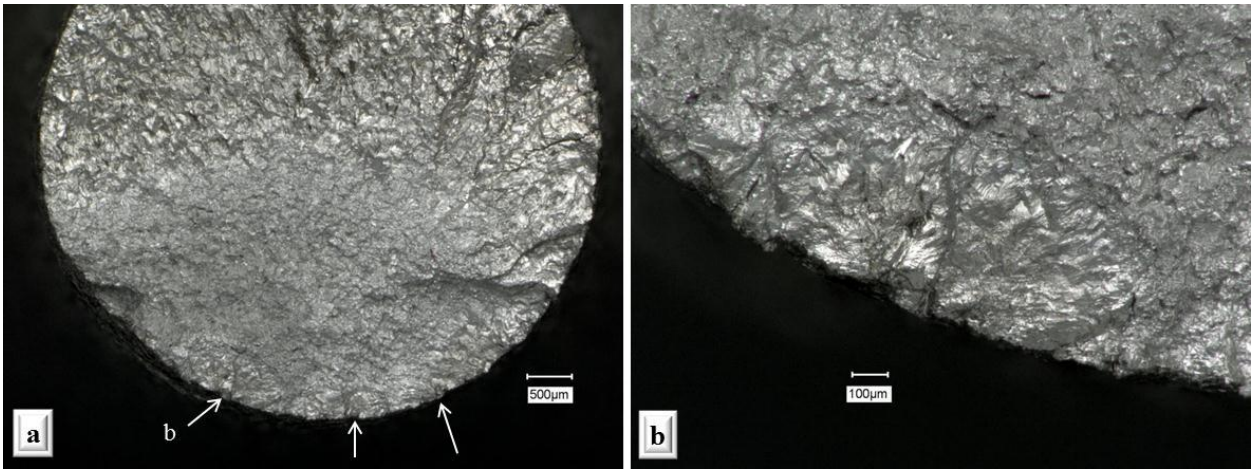

Figure 15: Fracture surface of vertically-built, HIP'd DMLS 316L fatigue specimen; (a) non-planar surface formed from linkage of several discrete fatigue cracks initiating at surface defects (b).

Results from fatigue tests conducted with 17-4PH specimens are plotted in Figure 16. Fatigue strength displayed by the wrought material was nearly 900 MPa in the low-cycle regime, and decreased in log- linear fashion to an apparent endurance limit of about 450 MPa. DMLS specimens fabricated in the horizontal orientation produced nearly the same fatigue strength as conventional material, but with more noticeable scatter. The first batch of DMLS 17-4PH specimens built in the vertical orientation (thus

stressed across the build planes in these tests) demonstrated cyclic fatigue strengths of approximaely 60% of those measured with wrought material. A second batch of vertically-built DMLS 17-4PH produced much poorer fatigue behavior, displaying only about 25% of the fatigue strength of both wrought and DMLS materials built in the horizontal orientation. Brief inspection of the fracture surfaces in the two batches of vertically-built specimens (shown in subsequent figures) indicates significant differences in the laser-fusion process must have occurred, though records corresponding to the fabrication jobs do not reveal any inconsistency.

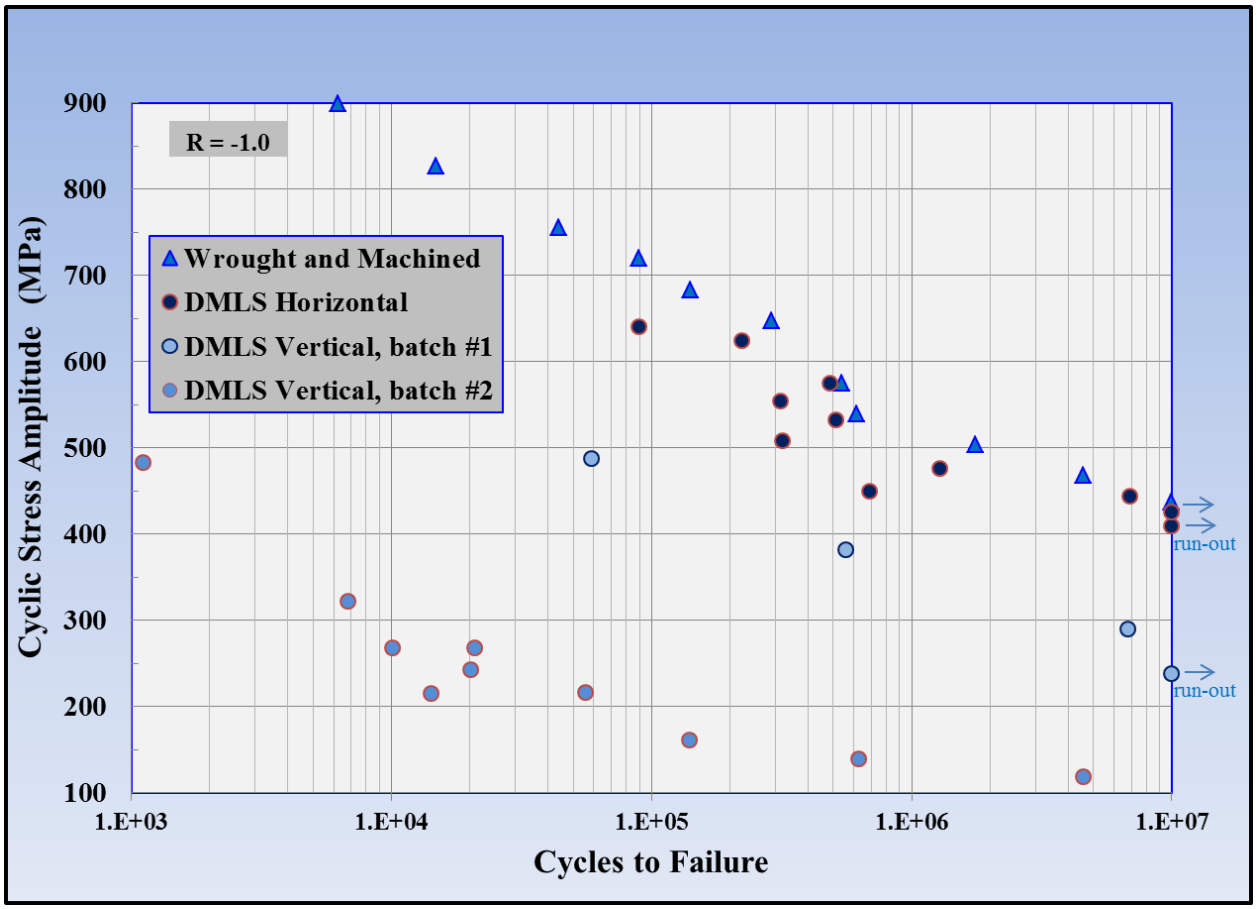

Figure 16: Measured room-temperature stress-life (S-N) of DMLS 17-4PH, compared to that of conventional material. Bending fatigue (rotating beam) at a frequency of 25 Hz.

DMLS 17-4PH materials produced in the horizontal orientation generated fatigue fractures that often were nearly planar with traces of the laser path evident, as shown in Figure 17a, even though the principal stress during testing was parallel to the build planes of these specimens. In some instances the fracture surface was rougher, with evidence of plastic flow radiating from the initiation site as shown in Figure 18b. On this fracture surface, the transition from fatigue growth to final rupture can be seen clearly (in Fig. 18a) by the change in surface reflectivity The fatigue cracks in all of the DMLS 17-4PH specimens built horizontally initiated at subsurface voids, as shown in Figures 17b and 18b.

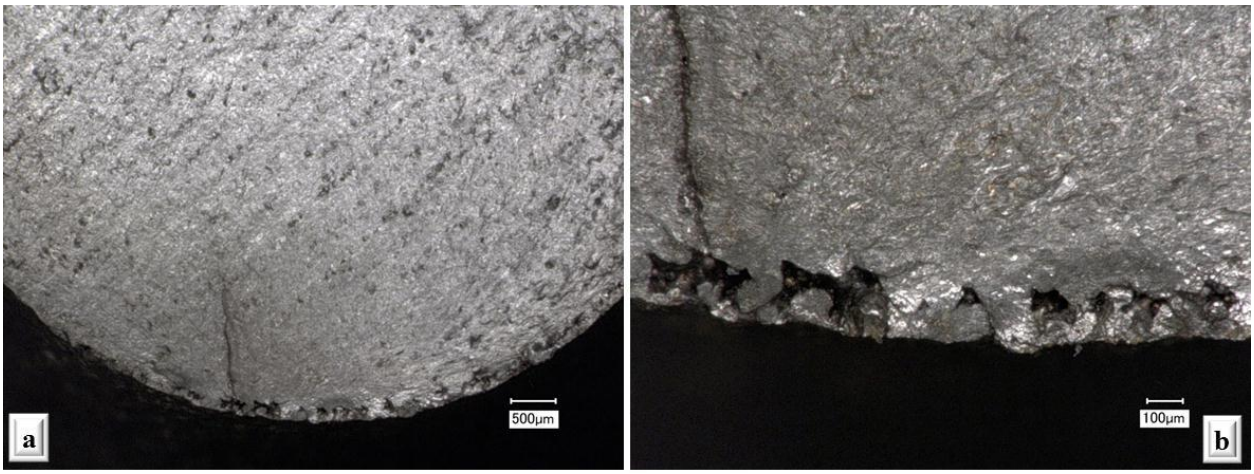

Figure 17: Fracture surface of DMLS 17-4PH horizontally-built fatigue specimen; (a) nearly planar surface with laser paths evident, and (b) initiation at surface pits and subsurface defects.

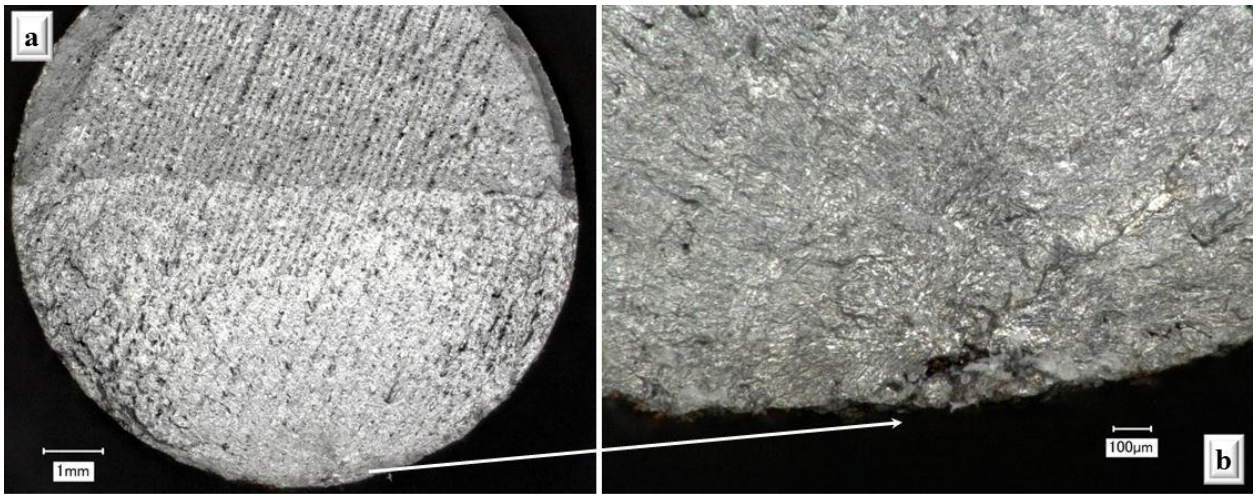

Figure 18: Fracture surface of DMLS 17-4PH horizontally-built fatigue specimen; (a) rougher surface with clear transition from fatigue to final rupture, and (b) initiation at subsurface voids.

Surface defects in the first batch of vertically-built DMLS 17-4PH fatigue specimens were relatively benign, such that cracks initiated at dominant, internal defects as shown in Figure 19a, b, d. These materials appeared to be completely fused, with no laser traces or segregated beads of melted and solidified powder evident on the surface. Fracture surfaces were rough and tortuous, indicative of ductile growth as displayed in Figure 20c. In stark contrast, fracture surfaces of specimens from the second batch of vertically-built material showed clear evidence of incomplete fusion. The fracture surface shown in Figure 19a suggests that specimen separated precisely between two build planes, and shows many artifacts of the laser path. The view with higher magnificaiton in Figure 20b reveals segements of material that had been melted, pressed flat against a solid, and solidified without fusing. Also abundantly evident are beads of solidified powder that had been melted but not fused by the laser. These features may be seen more clearly, along with several large pores, in the three-dimensional enlargement in Figure 21.

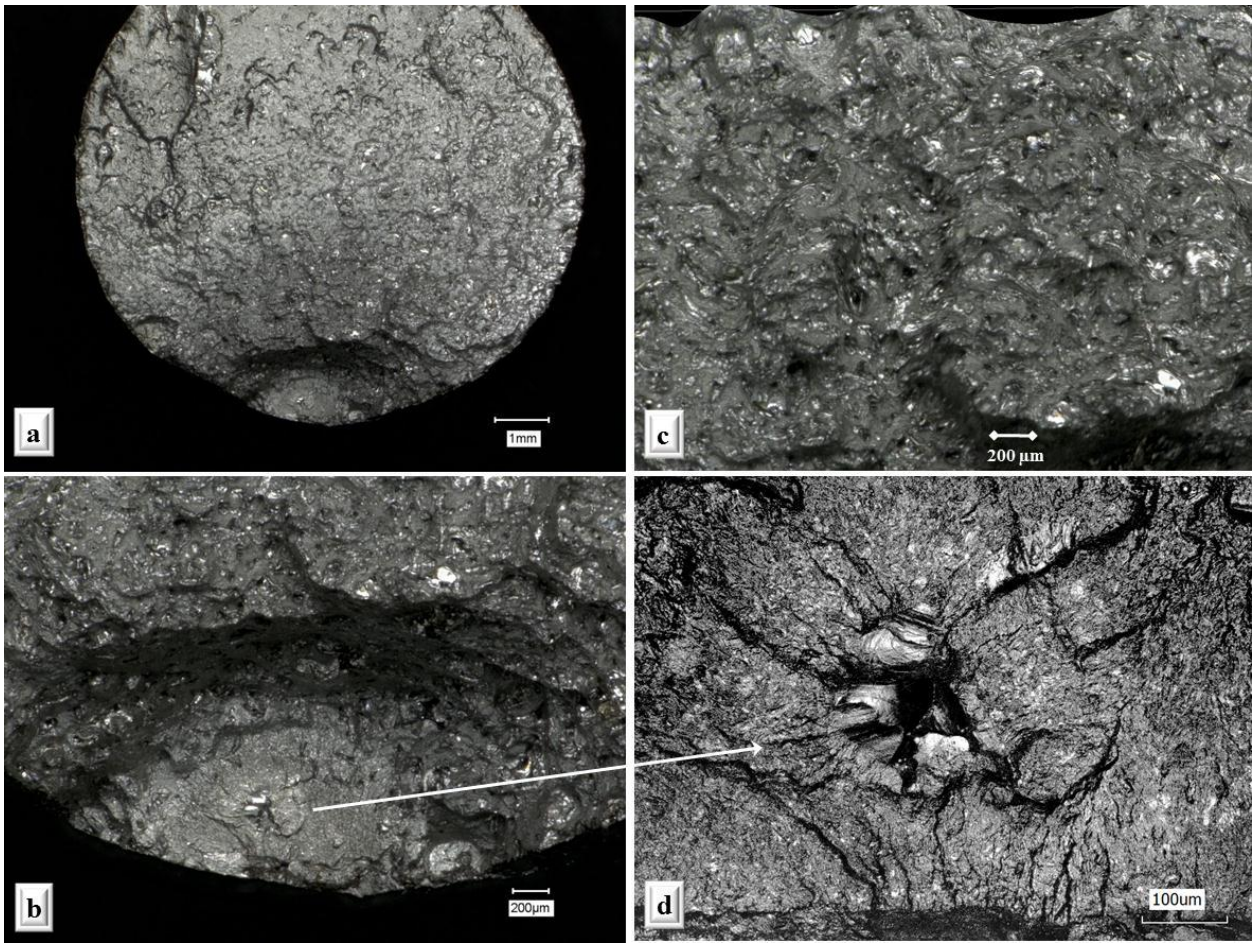

Figure 19: Fatigue fracture of specimen from first batch of DMLS 17-4 fabricated vertically, with initiation at interior defect, and rough fracture surface demonstrating fully fused material.

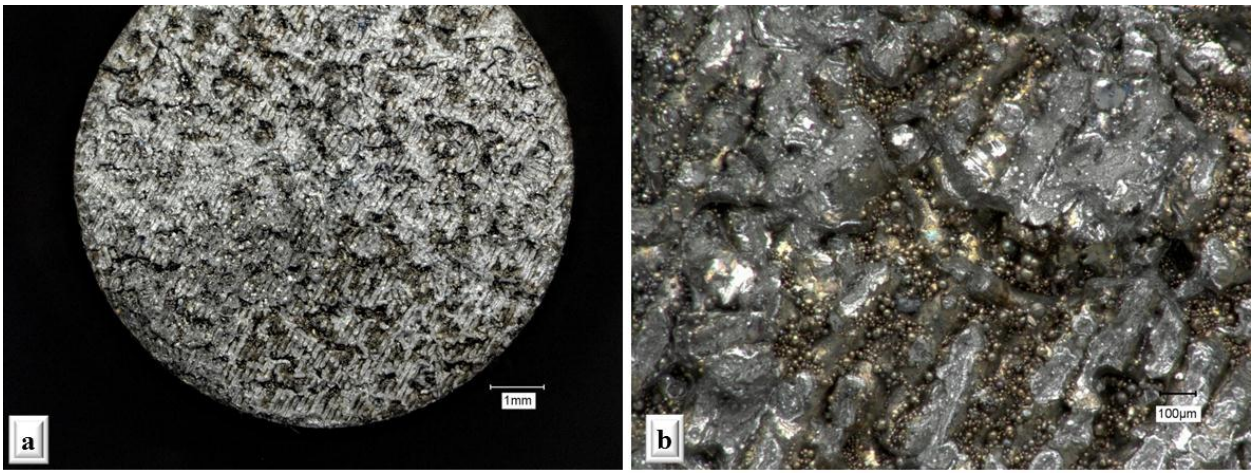

Figure 20: Fracture surface from second batch of vertically-built DMLS 17-4PH fatigue specimens; (a) planar surface with incomplete fusion evident, and (b) re-solidified powder beads, several pores.

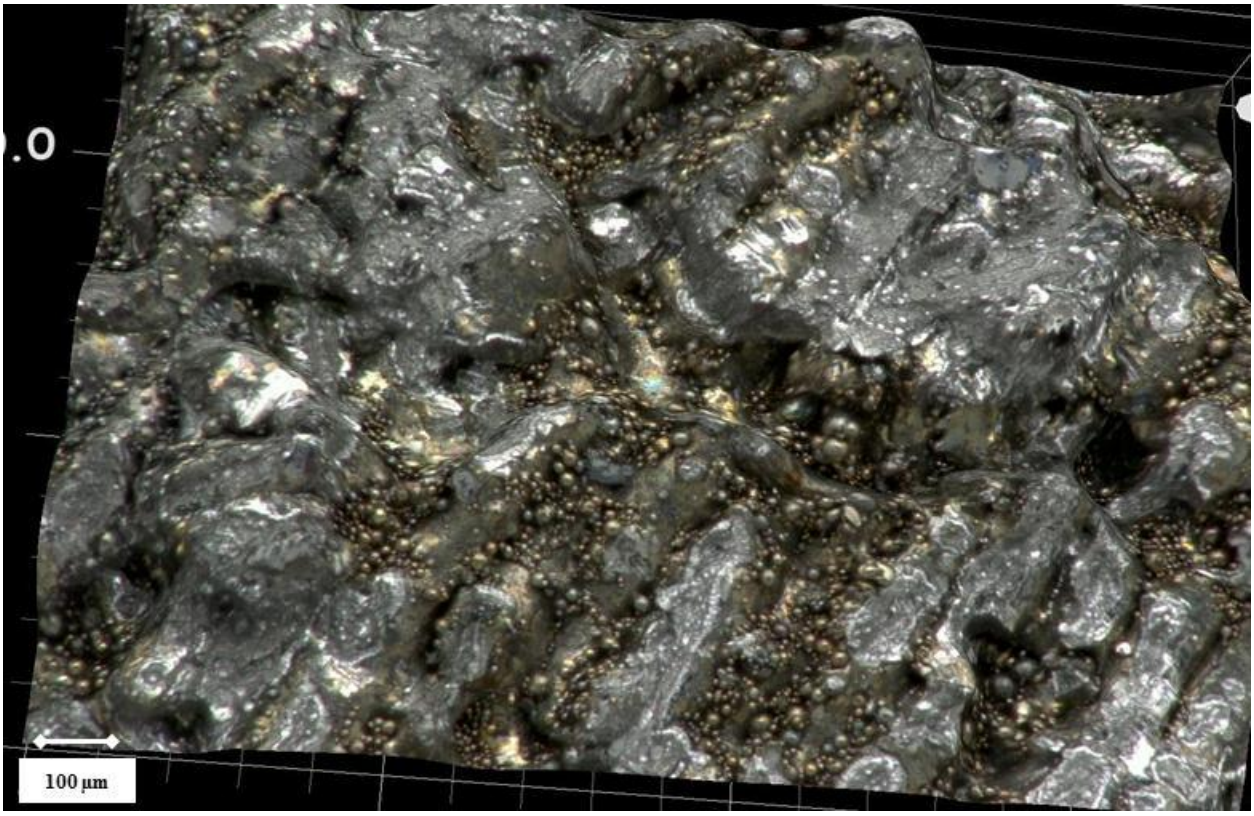

Figure 21: Three-dimensional reproduction of image in Figure 20, showing more clearly the melted but incompletely fused powder, distinctly defined laser paths and large voids.

4. Discussion

4.1 Quasi-static behavior

The elastic behavior of the DMLS stainless steels investigated here is quite comparable to that of conventional, wrought materials. The DMLS 316L materials produced in the horizontal and the inclined orientations displayed flexural moduli of approximately 187 and 189 GPa, respectively, compared to 191 GPa for the wrought, annealed material. Similarly, the flex modulus of DMLS 17-4PH in the inclined position (193 GPa) was nearly equal to that of wrought material (194 GPa). Stiffness of the DMLS 17-4 in the horizontal orientation was about 10% lower (172 GPa).

High ductility was exhibited by DMLS 316L during tensile-deformation measurements, reaching elongations of approximately 30% at failure. These materials yielded at stresses much higher than the yield stress of wrought, annealed 316L (345 MPa): when tested with the principal stress aligned with the build planes, specimens (built horizontally) yielded at about 496 MPa; specimens fabricated in the 45-degree inclined position produced an average yield stress of approximately 473 MPa. The higher yield stress displayed by the DMLS materials can be attributed to the fine crystalline structure created by the rapid solidification during the process of building the material in thin, discrete layers. The tensile yield stress measured in DMLS 17-4PH materials was significantly lower than that displayed by wrought material in the mill-annealed condition (~900 MPa). Yielding in specimens built horizontally occurred at about 610 MPa, whereas the average yield stress in specimens built at a 45-degree incline was 737 MPa. This difference in strength suggests the two materials may have different microstructures, which is substantiated by a closer look at the enlarged photomicrographs reproduced in Figure 22.

While the DMLS 17-4PH material fabricated in the horizontal orientation has fine, evenly distributed grains, material created with the specimen built on a 45-degree incline appears very different. This material presents a structure composed of groups of layered formations, suggesting they are martensitic lamellae within remaining austenite [18], formed during brief cooling cycles while the material was additively built. A similar-looking 17-4PH microstructure was described by Deng et al. as martensitic laths within austenite [19]. The difference in microstructure within materials produced in two different orientations but otherwise using

nominally similar parameters in the DMLS process provides compelling evidence that further study should be focused upon the evolution of microstructure in DMLS materials. (We note that it is likely that the maximum temperature and cooling rates were different during the two fabrication processes.)

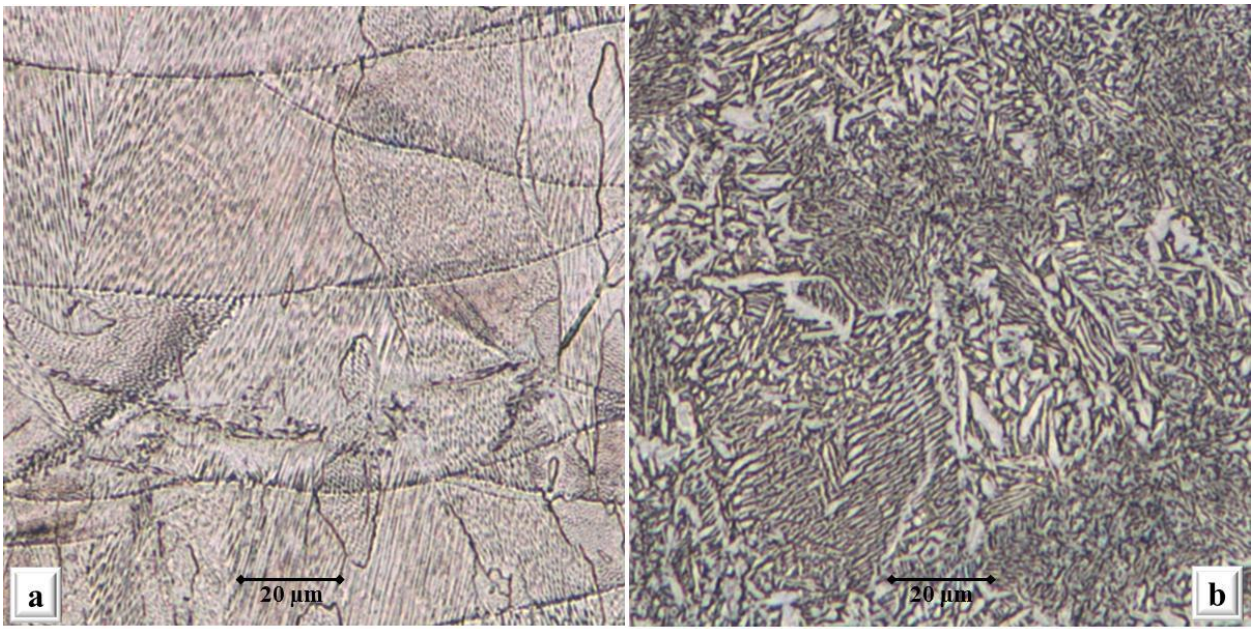

Figure 22: Microstructure of DMLS 17-4; (a) horizontally built, and (b) built on a 45° incline.

4.2 Cyclic fatigue behavior

Cyclic fatigue strengths demonstrated by the DMLS stainless steels fabricated in the horizontal orientation were almost equal to those of the corresponding wrought materials. Greater scatter produced by the DMLS specimens results from the prevalence of defects in these materials, both on the surface as well as throughout the bulk. Note that since the fatigue testing was performed in a bending configuration, axial stresses were produced which were aligned with the build planes of the horizontally-built specimens. In contrast, DMLS materials fabricated in the vertical orientation were subjected to tensile stresses applied perpendicular to (across) the build planes, and displayed significantly lower fatigue strengths.

The conventional (wrought, annealed, machined and polished) 316L material studied here displayed a fatigue strength of 350 MPa at 10^5 cycles, which agrees well with the result reported (~380 MPa) by Puchi-Cabrera et al. for similar conditions [20]. The lower value here is consistent with our lower measured ultimate stress (563 MPa) compared to 700 MPa reported by Puchi-Cabrera. DMLS 316L specimens built vertically, in two separate fabrication runs, produced fatigue strengths at lifetimes of 10^5 to 10^6 cycles of only about 30% of that generated by horizontally-built DMLS material. In response to a cyclic stress amplitude of 110 MPa, our vertically-built 316L failed at a little over 10^6 cycles, which compares quite well to a lifetime of $2x10^6$ cycles reported by Riemer et al. for similar, vertically-built material in the as-fabricated condition, tested with R=-1 in axial fatigue [16]. Machining the surface of their specimens raised the reported fatigue strength significantly (at $2x10^6$ cycles), to 267 MPa. Subjecting their turned specimens to HIP increased the fatigue strength by approximately 20%, to 317 MPa. Because post machining materials produced additively negates the very feature that makes the manufacturing technique attractive, we treated as-built specimens to HIP to investigate whether that process could enhance the fatigue life of vertically-built DMLS materials (by possibly ameliorating the effects of intrinsic defects and potential incomplete fusion between build planes). As indicated in Figure 12, the fatigue tests demonstrated an improvement in high-cycle fatigue strength but had little discernable impact upon low-cycle behavior. This result may be explained by the HIP process reducing the prevalence of smaller-sized defects that initiate cracks at high cyclic lifetimes, but having little effect upon the larger defects that govern the high stress, low-cycle fatigue behavior. Although the HIP temperature was nearly 200°C below the melting temperature of 316L, it may be possible that the HIP process effectively fused layers together more completely, as evidenced by rougher, non-planar fracture surfaces in the HIP'd materials.

Two separate batches of vertically-built, DMLS 17-4PH fatigue specimens were also tested, with disparate results. One batch of these materials exhibited fatigue strengths of about 25% of those of horizontally-built material. In these specimens, fracture surfaces displayed definitive evidence that the layered manufacturing process achieved incomplete fusion of material across the build planes, causing an intrinsic weakness responsible for the very low fatigue strengths observed. The second batch of vertically-built 17-4PH materials produced distinctly improved cyclic fatigue behavior, with fatigue strengths of about 75% of that generated

by horizontally-built materials. Fracture surfaces of these specimens indicated that complete melting and fusion of the powder had occurred during the fabrication process. Since no differences were observed on the exterior surfaces of these two batches of ostensibly identical materials, an important concern arises: How will end-users and providers of DMLS fabrication services develop assurance that components created with this AM process possess optimal material properties? This issue appears to be of greatest significance for products that will be exposed to dynamic mechanical loads, since fatigue failures are most often not accompanied by gradual signs of declining health.

It should be emphasized that the fatigue behavior of DMLS materials with as-fabricated surfaces has significant relevance to the application of components produced with DMLS, since the AM process enables fabrication of complex parts that cannot be post-machined. Additionally, testing in fully reversed bending represents the most severe cyclic fatigue condition for materials which possess high populations of surface defects and for which surface polishing is not a possible option.

5. Summary

The mechanical behavior of two stainless steels, 316L and 17-4PH, fabricated with direct metal laser sintering in two build orientations was measured and compared to that of conventional, wrought and machined materials. Measured flexural moduli were similar between the additively-manufactured and conventional materials. High ductility in the DMLS 316L was demonstrated in tensile deformation measurements, with considerably higher yield strength and strain hardening than in wrought, annealed 316L. In contrast, yielding of the DMLS 17-4PH materials fabricated both horizontally and at a 45-degree incline occurred at lower values than in the conventional material.

Surface roughness measurements indicated that the DMLS specimens were 5 to 8 times rougher than wrought, machined and polished specimens. DMLS microstructures generally revealed very small grains and a low population of pores up to 10 μm in diameter. It was revealed that unknown or seemingly insignificant differences in process parameters can result in creation of material microstructures with distinctly dissimilar characteristics.

Cyclic fatigue-strength measurements were conducted in fully-reversed, rotating bending. These tests demonstrated DMLS 316L and 17-4PH materials fabricated in the horizontal orientation have between 85 and 95% of the fatigue strength of corresponding wrought materials. Fatigue fractures in the DMLS materials were initiated at surface pits and subsurface voids, which are responsible for modest scatter in the data. Vertically-built DMLS materials are prone to fatigue fractures developing prematurely by separation of the material across the build planes, resulting in significantly reduced fatigue strengths. In the case of 316L, two separate batches of vertically-built specimens reinforced the existence of this behavior and therefore the need to consider post-processing methods to reduce its severity. Hot isostatic pressure was applied to another batch of vertically-built DMLS 316L specimens, which displayed improved high-cycle fatigue behavior but no enhancement of high-amplitude fatigue life. In the case of 17-4PH, distinctly different fatigue behaviors in two batches of vertically-built specimens stemmed from incomplete fusion between material layers in the inferior batch. These results demonstrate that, although the quasi-static mechanical behavior of DMLS materials compares favorably with that of conventional materials, concern remains about assuring that DMLS processing parameters are controlled well enough to provide adequate fatigue strength for dynamic applications.

6. Acknowledgement

This work is sponsored by the Department of the Air Force under the United States Air Force contract number FA8721-05-C-0002. The opinions, interpretations, recommendations and conclusions are those of the authors and are not necessarily endorsed by the United States Government. Donation of follow-on batches of fatigue specimens by Linear Mold and Engineering is gratefully acknowledged.

7. References

[1] Gu, D.D., Meiners, W., Wissenbach, K. and Roprawe, R. Laser additive manufacturing of metallic components: materials, processes and mechanisms. International Materials Reviews 2012; 57(3):133-164.

[2] ASTM Standard F2792, 2012a. Standard Terminology for Additive Manufacturing Technologies. ASTM International, West Conshohocken, PA.

[3] Manfredi, D. et al., Additive manufacturing of Al Alloys and aluminum matrix composites (AMCs). in Light Metal Alloys Applications, Monteiro (ed.), InTech ISBN 978-953-51-1588-5.

[4] Krishnan M. Investigation of material and mechanical properties of Al alloy and Al based MMC parts produced by DMLS for industrial application. PhD Thesis. Politecnico di Torino; 2014.

[5] Buchbinder, D., Schleifenbaum, H., Heidrich, S., Meiners, W. and Bültmann, J. High power selective laser melting (HP SLM) of aluminum parts. Phys. Procedia 2011; (12): 271–278.

[6] Kempen, K., Thijs, L., Yasa, E., Badrosamay, M., Verheecke, W. and Kruth, J.-P. Mechanical properties of AlSi10Mg produced by selective laser melting.

[7] Brandl, E., Leyens, C. and Palm, F., Schoberth, A. and Onteniente, P. Wire instead of powder? Properties of additive manufactured Ti-6Al-4V for aerospace applications. Euro-uRapid Intn'l. Conf. on Rapid Prototyping, Rapid Tooling & Rapid Manufacturing 2008; Berlin, Germany.

[8] Van Hooreweder, B., Boonen, R., Moens, D., Kruth, J.-P. and Sas, P. On the determination of fatigue properties of Ti6Al4V produced by selective laser melting. Proceedings of the 53rd AIAA/ASME Structures, Structural Dynamics and Materials Conference 2012; Honolulu, Hawaii.

[9] Leuders, S., Thöne, M., Riemer, A., Niendorf, T., Tröster, T., Richard, H.A. and Maier, H.J. On the mechanical behavior of titanium alloy Ti6Al4V manufactured by selective laser melting: Fatigue resistance and crack-growth performance. International Journal of Fatigue 2013; 48:300-307.

[10] Liu, Q., Elambasseril, J., Sun, S., Leary, M., Brandt, M. and Sharp, P.K. The effect of manufacturing defects on the fatigue behavior of Ti-6Al-4V specimens fabricated using selective laser melting. Advanced Materials Research 2014; (891-892): 1519-1524.

[11] Chan, K.S., Koike, M., Mason, R.L. and Okabe, T. Fatigue life of titanium alloys fabricated by additive layer manufacturing techniques for dental implants. Metallurgical and Materials Transactions A 2013; (44A): 1010-1022.

[12] Edwards, P. and Ramulu, M. Fatigue performance of selective laser melted Ti-6Al-4V. Materials Science and Engineering A 2014; (598): 327-337.

[13] Rafi, H.K., Starr, T.L. and Stucker, B.E. A comparison of the tensile, fatigue and fracture behavior of Ti-6Al-4V and 15-5 PH stainless steel parts made by selective laser melting. International Journal of Manufacturing Technology 2013; (69): 1299-1309.

[14] Spierings, A.B., Starr, T.L. and Wegener, K. Fatigue performance of additive manufactured metallic parts. Rapid Prototyping Journal 2013; 19(2): 88-94.

[15] Yasa, E. and Kruth, J.-P. Microstructural investigation of Selective Laser Melting 316L stainless steel parts exposed to laser re-melting. Procedia Engineering 2011; 19:389-395.

[16] Riemer, A., Leuders, S., Thone, M., Richard, H.A., Troster, T. and Niendorf, T. On the fatigue crack growth behavior in 316L stainless steel manufactured by selective laser melting. Engineering Fracture Mechanics 2014; 120: 15-25.

[17] Murr, L.E., Martinez, E., Hernandez, J., Collins, S., Amato, K.N., Gaytan, S.M. and Shindo, P.W. Microstructures and properties of 17-4 PH stainless steel fabricated by selective laser melting. J. Materials Research and Technology 2012; 1(3):167-177.

[18] Smallman, R.E. and Ngan, A.H.W. Physical metallurgy and advanced materials. Elsevier, Oxford; 2007:416-420.

[19] Deng, D., Chen, R., Sun, Q. and Li, X. Microstructural study of 17-4PH stainless steel after plasma-transferred arc welding. Materials 2015; 8: 424-434.

[20] Puchi-Cabrera, E.S., Matínez, F., Herrera, I., Berríos, J.A., Dixit, S. and Bhat, D. On the fatigue behavior of an AISI 316L stainless steel coated with a PVD TiN deposit. Surface and Coatings Technology 2004; 182: 276–286